

Recent Constraints on Models of Quintessence

M.Doran

Department of Physics & Astronomy, Dartmouth College, 6127 Wilder Laboratory, Hanover, NH 03755



We perform a comparison of the WMAP measurements with the predictions of quintessence cosmological models of dark energy. We consider a wide range of quintessence models, including: a constant equation-of-state; a simply-parametrized, time-evolving equation-of-state; a class of models of early quintessence; scalar fields with an inverse-power law potential. We also provide a joint fit to the CBI and ACBAR CMB data, and the type 1a supernovae.

1 Introduction

We carry out an extensive analysis¹ of the CMB anisotropy and mass fluctuation spectra for a wide range of quintessence^{2,3,4} models. These models are: (Q1) models with a constant equation-of-state, w , including $w < -1$; (Q2) models with a simply-parametrized, time-evolving w ; (Q3) early quintessence models, with a non-negligible energy density during the recombination era; (Q4) trackers described by a scalar field evolving under an inverse-power law potential.

The suite of parameters describing the cosmological models are split into quintessence parameters, θ_Q and spacetime plus “matter sector” variables, θ_M , where $\theta_M = \{\Omega_b h^2, \Omega_{cdm} h^2, h, n_s, A_S, \tau_r\}$. In order, these are the baryon density, cold dark matter density, hubble parameter, scalar perturbation spectral index, scalar perturbation amplitude, and optical depth. We restrict our attention to spatially-flat, cold dark matter models with a primordial spectrum of nearly scale-invariant density perturbations generated by inflation.

2 Constant w and phantom dark energy

For a constant equation of state, we have used the equivalence between a scalar field φ with potential $V(\varphi)$ and the equation-of-state w in order to self-consistently evaluate the quintessence fluctuations. For the range $w < -1$ we employ a k essence model, keeping the sound speed

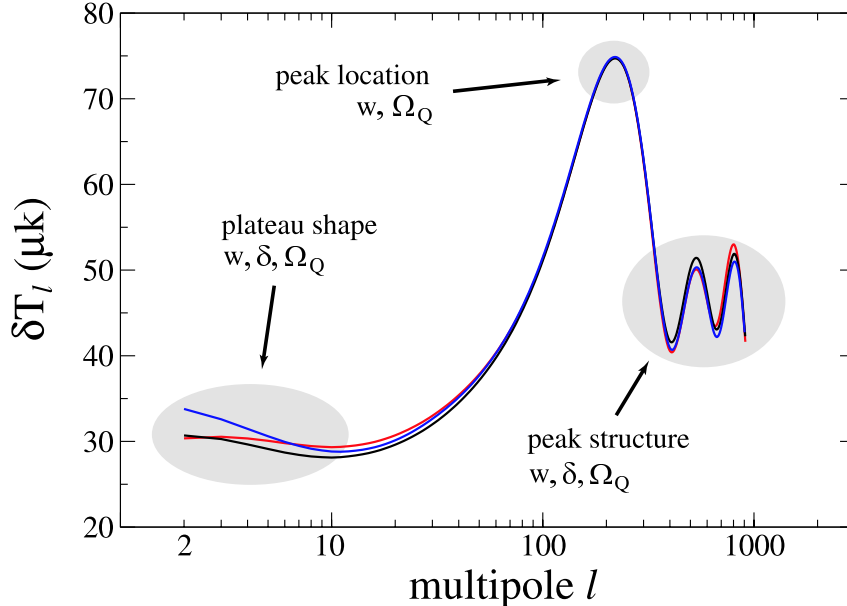


Figure 1: The pattern of CMB anisotropy can reveal information about the quintessence abundance (Ω_Q), equation-of-state (w), and behavior of fluctuations (δ). The three curves are examples of constant equation-of-state models which differ little by eye, but are distinguished by the data. The red ($w = -0.5$) and blue (-1.2) curves are both low- χ^2 CMB-indistinguishable, but distinct with respect to SNe. The black curve (-0.8), although it is consistent with the SNe data is rejected by the CMB at the 3σ -level.

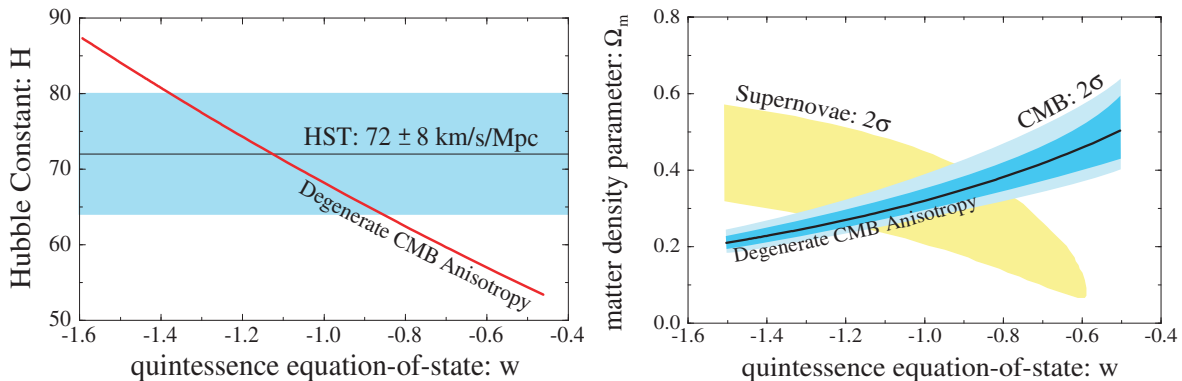
(actually, this is $d\omega^2/dk^2$) fixed at $c_s^2 = 1$. Since this model introduces only one additional parameter beyond the basic set of spacetime plus matter sector variables, we adopt a simplistic grid-based search for viable models. The acceptance criteria for the Q1 models is based on a $\Delta\chi^2$ -test. The results of our survey of Q1 models are shown in Figures 2(a), 2(b). Our basic conclusion from the overlapping constraint regions is that there exist concordant models with $-1.25 \lesssim w \lesssim -0.8$ and $0.25 \lesssim \Omega_m \lesssim 0.4$.

3 Celestine quintessence: $w(a) = w_0 + (1 - a)w_1$

We have examined quintessence models with an equation-of-state that evolves monotonically with the scale factor, as $w(a) = w_0 + (1 - a)w_1$. This parametrization has been shown to be versatile in describing the late-time quintessence evolution for a wide class of scalar field models⁵. Based on the degeneracy of models found for Q1, we expect to find a two-dimensional family of equivalent best-fit models with the same apparent angular size of the last scattering horizon, occupying a plane in the $\{w_0, w_1, h\}$ space. We find $w_0 < -0.75$ at the 2σ level, marginalizing over the suppressed five dimensional parameter space, as illustrated in Figure 2(c). There, the shapes of the contours indicate that current data can only distinguish between fast ($dw/da \gtrsim 0.5$) and slow evolution of $w(a)$, and offer only a weak bound on w_1 . However, in terms of Ω_Q^{ls} the relative quintessence density during recombination, we find $\Omega_Q^{ls} < 0.03$ at the 2σ level.

4 Leaping kinetic term quintessence

Leaping kinetic quintessence features a non-canonical kinetic term that undergoes a sharp transition at late times, leading to the current accelerated expansion⁶. At early times the field closely tracks the cosmological background with $w = 0$ during matter domination, appearing as early quintessence⁷ before undergoing a steep transition towards a strongly negative equation-



(a) The one-parameter family of best-fit models, which exploit the geometric degeneracy of the CMB anisotropy pattern, is shown as the thick, red curve in the $w - h$ plane. We have explored models in a six-dimensional cylinder in the parameter space surrounding this “best-fit line.” The HST-Key Project 1σ measurement of the Hubble constant is shown by the shaded band.

(b) The constraints on constant equation-of-state models due to CMB (WMAP, ACBAR, CBI) and type 1a supernovae (Hi-Z, SCP) are shown. The starting point for our parameter-search, the family of CMB-degenerate models, is shown by the thick, black line.

of-state by the present day. Since Ω_Q^{ls} is not tied as closely to the expansion rate sampled by the supernovae, compared to case Q2, the result is the weaker constraint $\Omega_Q^{ls} \lesssim 0.1$, as shown in Figure 2(d). Although the limit of a cosmological constant can be approached in this model, the presence of early quintessence will then require a sharp transition in the equation-of-state in order to reach $w \rightarrow -1$. Consequently, we bar models with $w \approx -1$ and non-negligible Ω_Q^{ls} , as displayed in Figure 2(d). Next, because early quintessence suppresses the growth of fluctuations on small scales compared to large scales, we find that comparable fluctuation spectra can be achieved by making a trade-off between n_s and Ω_Q^{ls} (see Figure 2(g)).

5 Inverse power law quintessence

Inverse-power law (IPL) models are the archetype quintessence models with tracking property and acceleration^{2,8,9}. The potential is given by $V \propto \varphi^{-\alpha}$, where the constant of proportionality is determined by Ω_Q . In certain supersymmetric QCD realizations of the IPL¹⁰, α is related to the numbers of color and flavors, and can take on a continuous range of values $\alpha > 0$. For $\alpha \rightarrow 0$, however, inverse-power law models behave more and more like a cosmological constant. From our analysis, we see that $\alpha \lesssim 1 - 2$, only a minor improvement of earlier investigations^{11,12,13} using pre-WMAP data.

In Figure 2(h) we plot the likelihood contours in the $\Omega_m h^2 - \alpha$ plane: our results agree with the best fit at $\Omega_m h^2 = 0.149$ for $\alpha = 0$ or $w = -1$, but show a tolerance for a wider range for $0 \leq \alpha \leq 2$. That is, the additional degree of freedom in α means that the matter density for the IPL model is not as well-determined from the peak position¹⁴ as compared to the Λ model. However, to maintain the peak at $\ell = 220$, we observe that $\Omega_m h^2$ decreases slightly as α increases.

Acknowledgments

This work was supported by NSF grant PHY-0099543 at Dartmouth. We thank Pier Stefano Corasaniti for useful conversations, and Dartmouth colleagues Barrett Rogers and Brian Chaboyer for use of computing resources.

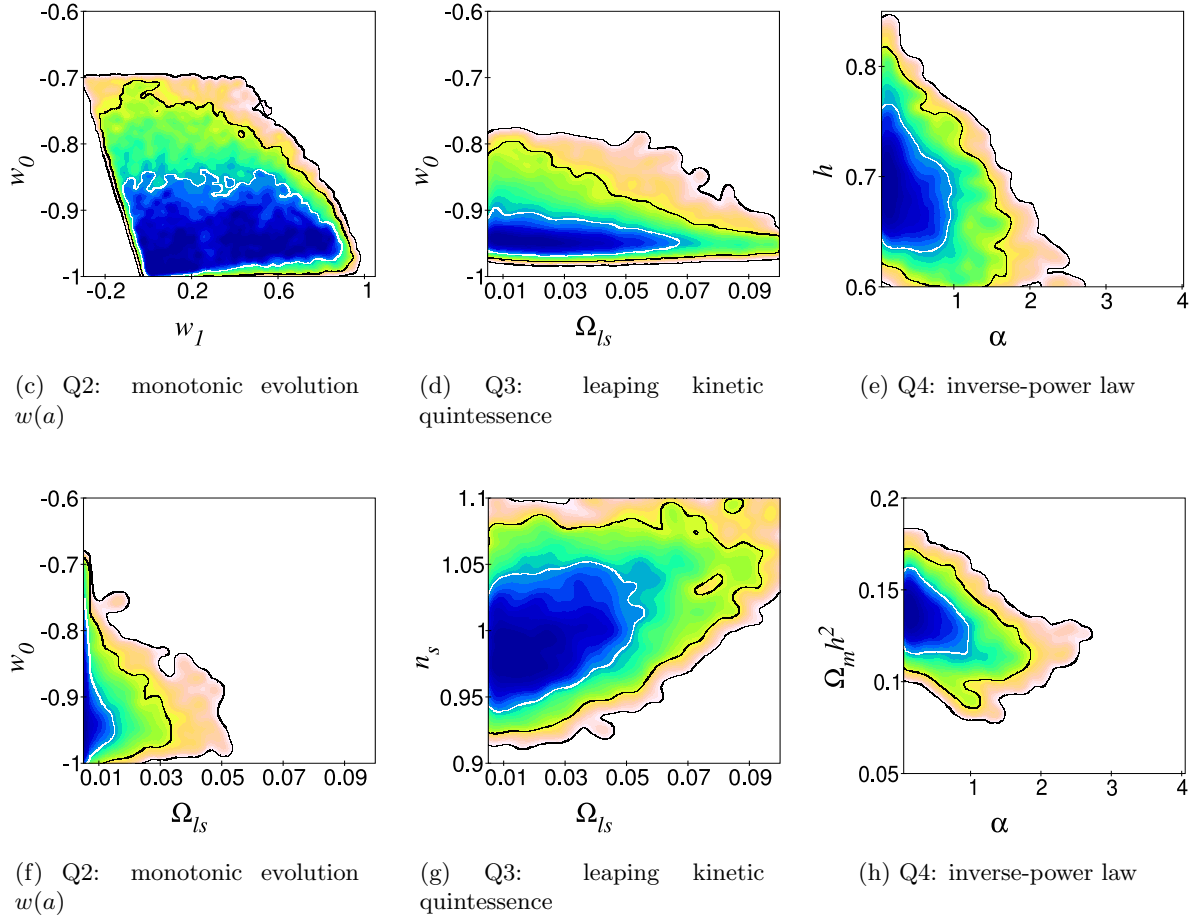


Figure 2: The results of our MCMC search of the multi-dimensional parameter search, for models Q2-4, are illustrated in the figures above. In all cases, we have marginalized over the suppressed parameters. The solid lines indicate the 1, 2, 3σ contours based on comparison with the CMB (WMAP, ACBAR, CBI) and type Ia supernovae (Hi-Z, SCP).

1. R. R. Caldwell and M. Doran, arXiv:astro-ph/0305334.
2. B. Ratra and P. J. Peebles, Phys. Rev. D **37**, 3406 (1988).
3. C. Wetterich, Nucl. Phys. B **302**, 668 (1988).
4. R. R. Caldwell, R. Dave and P. J. Steinhardt, Phys. Rev. Lett. **80**, 1582 (1998).
5. E. V. Linder, Phys. Rev. Lett. **90**, 091301 (2003).
6. A. Hebecker and C. Wetterich, Phys. Lett. B **497**, 281 (2001).
7. R. R. Caldwell, M. Doran, C. M. Mueller, G. Schaefer and C. Wetterich, [arXiv:astro-ph/0302505].
8. I. Zlatev, L. M. Wang and P. J. Steinhardt, Phys. Rev. Lett. **82**, 896 (1999).
9. P. J. Steinhardt, L. M. Wang and I. Zlatev, Phys. Rev. D **59**, 123504 (1999).
10. A. Masiero, M. Pietroni and F. Rosati, Phys. Rev. D **61**, 023504 (2000).
11. A. Balbi, C. Baccigalupi, S. Matarrese, F. Perrotta and N. Vittorio, Astrophys. J. **547**, L89 (2001).
12. C. Baccigalupi, A. Balbi, S. Matarrese, F. Perrotta and N. Vittorio, Phys. Rev. D **65**, 063520 (2002).
13. M. Doran, M. Lilley and C. Wetterich, Phys. Lett. B **528**, 175 (2002).
14. L. Page *et al.*, arXiv:astro-ph/0302220.